23rd Conference of the Italian Association of Aeronautics and Astronautics
AIDAA2015
Politecnico di Torino, 17-19 November 2015
E. Carrera, M. Cinefra, A. Pagani, M. Petrolo and E. Zappino (Editors)
www.aidaa2015.it

ANALYSIS OF TAPERED STRUCTURES BY MEANS OF REFINED 1D MODELS

Enrico Zappino*, Andrea Viglietti†, Erasmo Carrera*

Politecnico di Torino
Department of Mechanical and Aerospace Engineering
Corso Duca degli Abruzzi, 24
10129, Torino, Italy
*e-mail: enrico.zappino@polito.it, web page: http://www.mul2.com

†e-mail: andrea.viglietti@polito.it, web page: http://www.mul2.com

*e-mail: erasmo.carrera@polito.it, web page: http://www.mul2.com

Key words: CUF, One-dimensional model, tapered beam.

Summary. *This document presents the static analysis of reinforced tapered structures using 1D models. These models are based on one dimensional formulation derived through the unified formulation(CUF). This formulation provides 3D-like results thanks to the use of polynomial expansions to describe the displacement field over the cross-section. Depending on the types of expansion used, different classes of CUF are obtained. In this work the Lagrange expansions were used. The use of LE models allows each structural component to be considered separately; this approach is called component wise (CW). Different kind of aeronautical structures, gradually more complex, were studied. The stress and displacement fields due to simple load cases were obtained. The results have been compared with those obtained using commercial tools, 3D and 2D models have been used as comparisons. These last use solid and shell elements. The results show the capability of the present refined 1D models to achieve results usually obtained by use of solid models and therefore, with higher computational cost.*

1. INTRODUCTION

The typical aeronautical structures are composed by reinforced thin shell, in order to minimize the weight without reducing the performances. These structures are composed by skin (several panels joined), longitudinal stiffening spar and the transversal stiffener called ribs. The analysis of these thin-walled structures can be obtained by the use of classical methods discussed in [1][2]. The classical approaches assume constant shear stress inside panels. In order to overcome the limitations related to constant shear stress, the use of matrix methods was introduced by Argyris and Kensley [3]. These methods are automatic and are at the basis of the development of finite element methods (FEMs).

With the introduction of computational tools that implement the finite elements methods, the analysis of aircraft structures can be made using three elements typically: the solid (three-dimensional), the plate (two-dimensional) and the beam elements (one dimensional). One of the most popular software based on this approach is NASTRAN. Usually, solid elements are used for aerospace structures that lead to a huge computational cost. This is a complication when a multi-field problem is performed, as an aeroelastic or thermal analysis, or when a particular material are used, such as composite.

In order to overcome this issue, a equivalent lower-fidelity model is used. The most simplified model is called stick-model and concerns the use of one-dimensional model along the wing's elastic axis. This type of model implies the evaluation of the structural stiffness of the wing respect to its principal axes. Another approach is the 2D model. This last is useful to describe the several types of thin-walled structures which can be found in the aeronautical field. In conclusion, the structural analyses require a huge computational cost or a model with poor accuracy.

In this scenario, the development of *High fidelity reduced* models with very good accuracy is crucial, above all because the aeronautic structures are even more complex, both in the design field and in the material field.

In this work a refined 1D model based on Carrera Unified Formulation is applied. CUF has been developed for shell and plate theories by [4]. In the last years, the CUF has been extended to beam theories [5]. In general two classes of 1-D models were proposed: one based on the Taylor expansion (TE) and the other one based on the Lagrange Expansion (LE). Lately other expansions have been implemented as shown in [8][9] where, for example, trigonometric expansions were introduced. The LE models, used in this document, have only displacements as unknowns and this feature allows to impose the congruence between different structures without incurring in coupling issues. In this way each generic component of a reinforced shell structure has its 1D formulation.

This document can be subdivided into three parts. In the first a brief introduction at Unified Formulation is presented. Then the structures studied are shown and the results are reported. Finally, the main conclusions are highlighted.

2. 1-D Carrera Unified Formulation

In this section are provided some notions about the CUF. Initially, a brief introduction to the theory of structures is presented, followed by the description of the CUF and LE beam. Then the solution with the finite element is illustrated.

2.1 Preliminaries

For each general point the displacement vector can be identified:

$$\mathbf{u}^T = (u_x,\, u_y,\, u_z) \tag{1}$$

where u_x, u_y and u_z are the components along the three directions. The strains and stresses vectors are defined as:

$$\boldsymbol{\epsilon}^T = (\epsilon_{xx}, \epsilon_{yy}, \epsilon_{zz}, \epsilon_{xy}, \epsilon_{xz}, \epsilon_{yz}), \tag{2}$$

$$\boldsymbol{\sigma}^T = (\sigma_{xx}, \sigma_{yy}, \sigma_{zz}, \tau_{xy}, \tau_{xz}, \tau_{yz}). \tag{3}$$

The strain vector can be obtained using the differential operator **b**:

$$\boldsymbol{\epsilon} = \mathbf{bu}. \tag{4}$$

The extended form of **b** can be found in [6]. The Hooke's law introduces the relation between the stress field and the strain one:

$$\boldsymbol{\sigma} = \mathbf{C}\boldsymbol{\epsilon}, \tag{5}$$

where **C** is the stiffness coefficients matrix of the material. In order to describe an isotropic material, the matrix **C** can be expressed as:

$$\boldsymbol{C} = \begin{bmatrix} C_{11} & C_{12} & C_{12} & 0 & 0 & 0 \\ C_{21} & C_{11} & C_{12} & 0 & 0 & 0 \\ C_{21} & C_{21} & C_{11} & 0 & 0 & 0 \\ 0 & 0 & 0 & C_{44} & 0 & 0 \\ 0 & 0 & 0 & 0 & C_{44} & 0 \\ 0 & 0 & 0 & 0 & 0 & C_{44} \end{bmatrix} \tag{6}$$

The coefficients are defined

$$C_{11} = 2G + \lambda \quad C_{12} = C_{21} = \lambda \quad C_{44} = G \tag{7}$$

$$G = \frac{E}{2(1+\nu)} \quad \lambda = \frac{\nu E}{(1+\nu)(1-2\nu)} \tag{8}$$

where E is Young's modulus, G is the shear modulus and ν is Poisson's ratio. λ and G are also called as Lamè coefficients.

2.2 Unified Formulation

The model used in this document introducing an approximation of the displacement field of the beam. A generic three-dimensional displacement field expressed as

$$\mathbf{u} = \mathbf{u}(x, y, z). \tag{9}$$

can be re-written as

$$\mathbf{u} = F_\tau(x, z)\mathbf{u}_\tau(y), \qquad \tau = 1, 2 \dots M, \tag{10}$$

where $\mathbf{u}_\tau$ is the displacement vector and the F_τ represents the expansion used to approximate the behaviour of the beam cross-section. M is the number of terms of the expansion. The type of Lagrange polynomials used in this work for built 1D high-order model is nine-point elements (L9). There are other types of polynomials like four-point elements (L4). These polynomials are expressed by an isoparametric formulation in order to deal with any shape geometries as shown in fig.1. The interpolation functions can be found in [7].

Once that the function are defined, for example, the displacement field of L9 element along x is given by

$$u_x = F_1 u_{x_1} + F_2 u_{x_2} + F_3 u_{x_3} \ldots + F_9 u_{x_9} \tag{11}$$

where $u_{x_1} \ldots u_{x_9}$ represent the component along x of the displacement field of each node of the L9 elements. In order to have a better refined model, the cross section can be discretized by more L-elements joined together as show in fig.1.

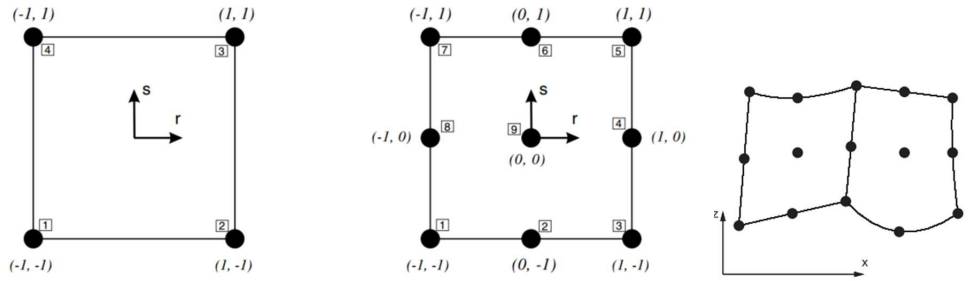

(a) L4 and L9 elements in natural reference system.

(b) Two assembled L9 in generic reference system.

Figure 1. L9.

2.3 Finite Element solution

In this part the FE solution based on Lagrange Expansion are going to be presented. The displacement vector is given by

$$\mathbf{u}(x, y, z) = F_\tau(x, z) N_i(y) \mathbf{q}_{\tau i} \tag{12}$$

where N_i are the shape functions and $\mathbf{q}_{\tau i}$ the nodal displacements vector. The B3 elements (elements with three nodes) are adopted in this work and the index i indicates the node of the beam element. The governing equations can be obtained using the PVD (Principle of Virtual Displacements) that, in the static case, is expressed as the equivalence between the work of the external loads (δL_{ext}) and the strain energy (δL_{int}). The term δ denotes the virtual variation.

$$\delta L_{int} = \delta L_{ext} \tag{13}$$

The internal work can be written as:

$$\delta L_{int} = \int_V \delta \boldsymbol{\epsilon}^T \boldsymbol{\sigma} dV \tag{14}$$

Introducing the Hooke's law and the geometrical relations, the internal work can be expressed in function of the N_i, the expansion used for the cross section and the properties of the material. The process to get the 15 can be found in [6].

$$\delta L_{int} = \delta \mathbf{q}_{sj} \int_V N_j(y) F_s(x,z) \mathbf{b}^T \mathbf{C} \mathbf{b} F_\tau(x,z) N_i(y) dV \mathbf{q}_{\tau i} \tag{15}$$

The stiffness matrix $\mathbf{K}^{ij\tau s}$ is obtained and it is expressed in term of *fundamental nucleus* (3×3 array).

In order to deepen the CUF, the TE and LE theory and its FE application, the recent book by Carrera et al. is suggested [6].

3. Numerical Results

In this section different aeronautical structures are examined. Initially the results of a simple reinforced panel are presented. First a rectangular panel is studied; then a tapered one is taken into account. In the second part a tapered wing box with rectangular cross section will be shown. The results are compared with those from a commercial FEM software. The software used is MSc/NASTRAN. Two model are used. The *solid model* was realized with 8-node element (HEX8) instead, the model called *shell+beam model* combines the two nodes beam elements (BAR2) for the stiffener and the plate elements (QUAD4) for the panels. The several structures presented in this section is made of a generic aluminium alloy with these properties: Young's module $E = 71.7\ GPa$, Poisson's ratio $\nu = 0.33$, density $\rho = 2810\ kg/m^3$.

3.1 Rectangular Shape

The first structure is a simple rectangular panel with two stiffeners along the biggest edge. One extremity is clamped and on the other one the load is applied. The geometrical data of the structure are the following: axial length $L = 1\ m$, panel height $h = 0.2\ m$, panel thickness $t = 0.002\ m$, stiffener cross-section $a \times b = 0.02 \times 0.02$. Figure 2 shows the several dimensions introduced. The force applied has a magnitude of $F = -50000\ N$.

The structure can be seen as the sum of three components: the stiffeners and the panel. The stiffeners are modeled in "typical method"; it means that the beam elements are along the length of the stiffener and the Lagrange Expansion is used to described the cross section. Instead, for the panel the thickness direction is taken as *beam axis*. The shape of the panel is discretized with the polynomial expansions. This method is going to be useful in order to model a tapered panel, as will be showed in the next section. In fig.2 these formulations are reported; the y axis identifies the direction of the beam elements. For the stiffeners are used 5 B3 elements (beam elements with three nodes). For the panel only one. During the analysis, a poor influence of the beam element number has been evaluated on the panel behaviour. For this reason only the

results with one beam element are presented. In order to have a better accuracy, the number of beam element along the stiffener can be increased (with an increase of the number of L9 elements for the panel cross-section) or can be introduced B4 beam elements.

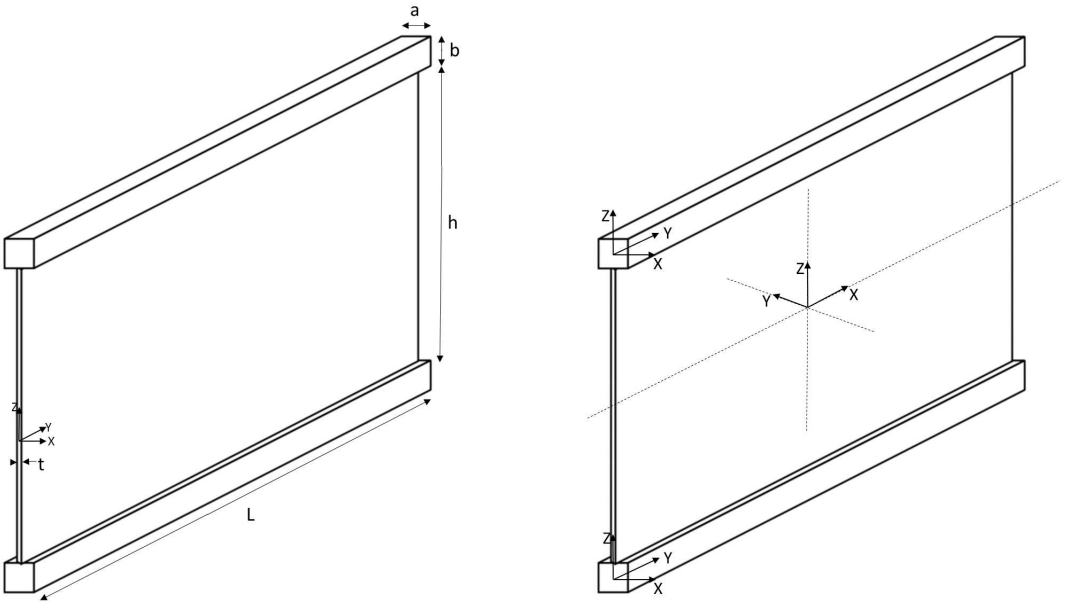

(a) Reinforced Panel (b) 1D formulation

Figure 2. Case analyzed.

In fig.3 the L9 distributions used for the cross-section are shown. In this case the two stiffeners have the same L9 distribution. This choice was adopted to simplify the assembling with the panel. In order to have also a *convergence analysis*, the panel was described with three different discretizations show in fig.3

The results are reported In the table 1.

Table 1. Average $\tau_{xz} \times 10^8$ on the rectangular panel at $y = L/2$ and $x = t/2$.

	BS	10 L9	20 L9	30 L9	Solid
DOF		3531	3927	4323	207993
$\tau_{xz}[Pa]$	-1.250	-1.114	-1.117	-1.117	-1.153

In fig.4 the values of shear stress along the panel height are showed.

It should be noted that the CUF approach provides results in agreement to those obtained with a solid model characterized by a significantly larger number of DOF. Moreover, the not constant shear stress distribution along the panel is confirmed.

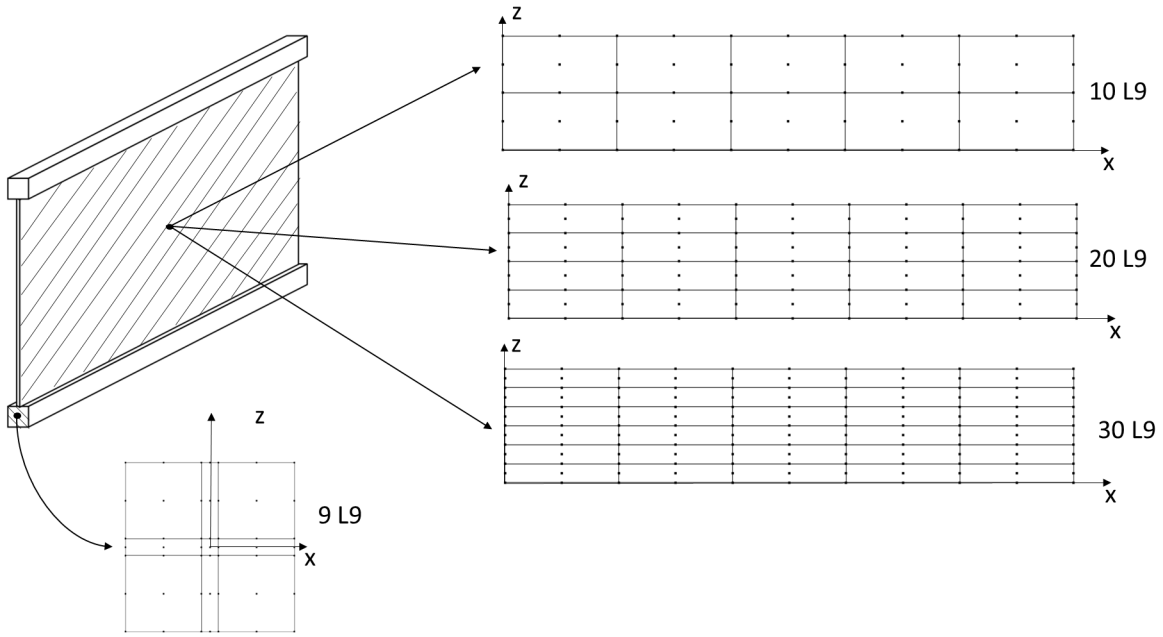

Figure 3. Cross-section L9 distributions for the rectangular structure.

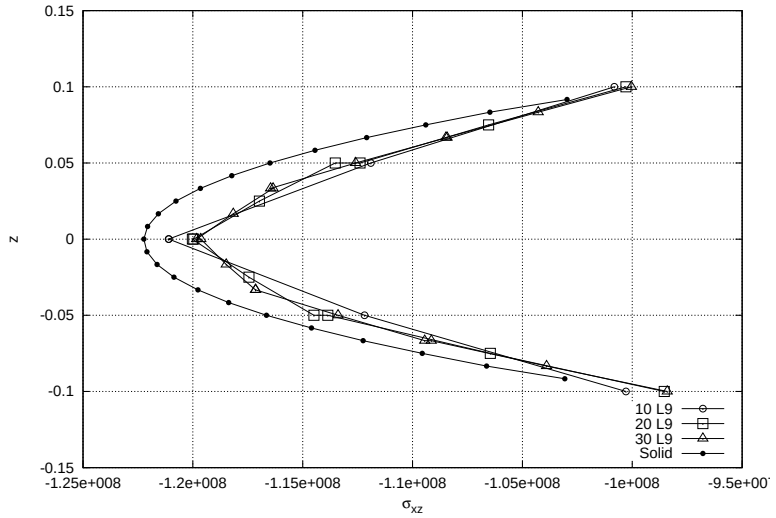

Figure 4. τ_{xz} vs z-axis at $L/2$ of the rectangular panel.

3.2 Tapered Shape

A tapered reinforced panel is now considered. Once again the beam axis is taken along the length to describe the stiffeners and along the thickness for the panel. The number of B3 elements used is the same of the previous model. For the panel formulation, considering the previous *assessment results*, only a discretization with 20 L9 is used, for a total of 99 points. The stiffener cross-section is the same of the previous one. Figure 6 presents the meshes used for the cross-sections. Using this approach, as the figure shows, the tapered panel is modeled with accuracy without introducing heavy approximations (for example the tapered edge approximated by *steps*). The length of the stiffener is always $L = 1\ m$, the bigger height of the panel is $h_1 = 0.2\ m$, the other one is obtained by rotating the stiffener. Introducing a taper angle of $\alpha = 2.5\ deg$, the value found is $h_2 = 0.1128\ m$. The panel thickness and the stiffener cross-section are the same of the precious case.The sizes are reported in fig.5 The force magnitude on the free extremity is equal to $F = -50000\ N$. The material used is the same aluminum alloy of the previous section.

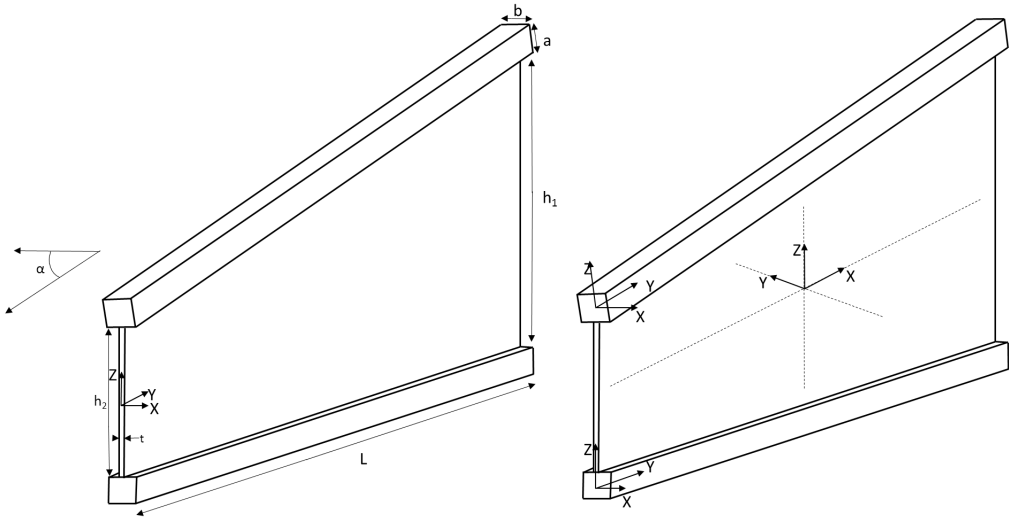

(a) Reinforced Panel (b) 1D formulation

Figure 5. Tapered formulation.

In the table 2 the displacement of two points are reported. The values are multiplied $\times 10^{-2}$. These two points match with the axis of the stiffeners at $L = 1\ [m]$. By reference to the fig.6 the points considered are located in local reference system at (0,L,0). w_a is related to upper stiffener where the load is applied. Instead w_b is related to lower stiffener.

In fig.7 the values of τ_{xz} along the height are shown instead the table n.1 shows the average values. The average value is evaluated in the middle plane of the panel.All the values are multiplied $\times 10^8$.

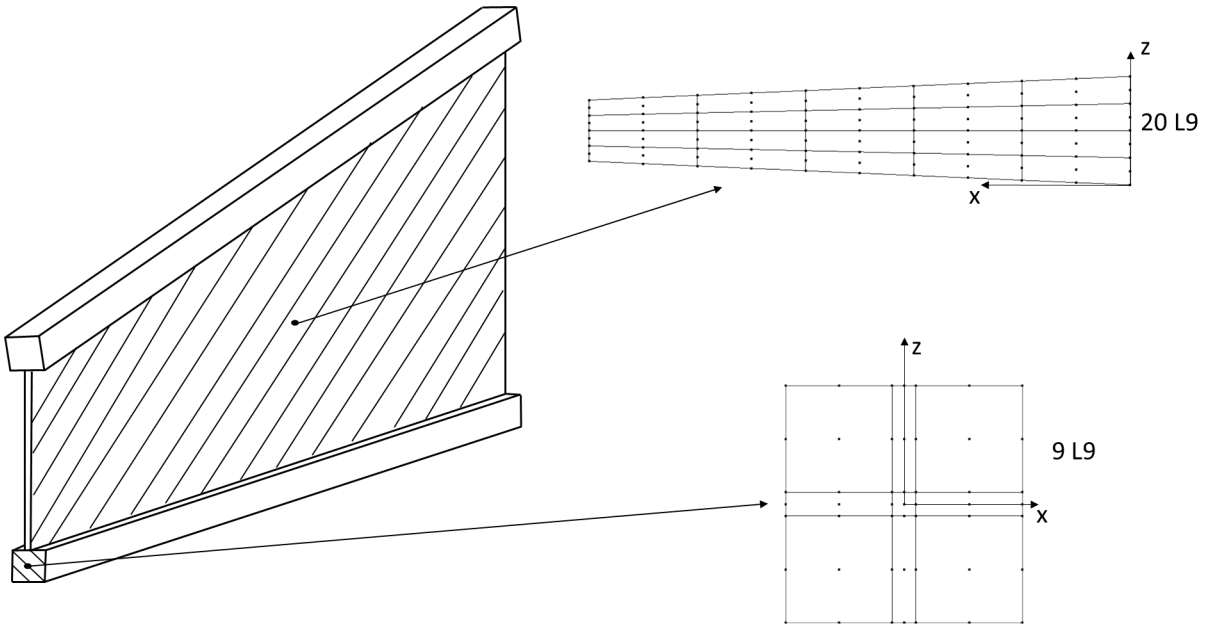

Figure 6. Cross-section L9 distributions for the tapered structure.

Table 2. w on the panel at $y = L/2$ and $x = t/2$.

Displacement	20L9	Solid	Shell+Beam
$w_a[m]$	-3.045	-3.049	-3.887
$w_b[m]$	-2.979	-2.973	-3.802

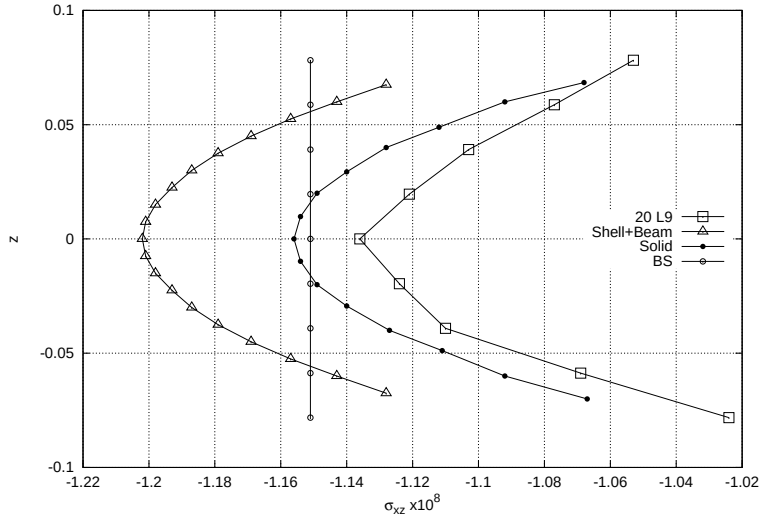

Figure 7. τ_{xz} vs z-axis at $L/2$.

Table 3. Average τ_{xz} on the panel at $y = L/2$ and $x = t/2$.

	BS	20 L9	Solid	Shell+Beam
DOF		3927	26019	4280
$\tau_{xz}[Pa]$	-1.151	-1.091	-1.123	-1.174

3.3 Tapered Wing Box

Now a tapered wing box is presented. The box is composed by eight elements, four stiffeners and four panels, numbered as shown in fig.8. At $y = L$ the structure is clamped and at $y = 0$ there is a load on stiffener n.2. The lenght is r_1 is $0.6\ m$ and $r_2 = 0.5218\ m$. The last data is due to the rotation of the stiffener around Z by an angle of $\alpha = 2.5\ deg$. The other geometrical data are those already introduced previously.

Table 4 shows the displacements of the four stiffeners at the tip. The points are located in the centre of the cross-section of the stiffener. The fig.10 shows the values of the shear stresses in the panel. The results of the BS are not reported because this model is not able to get accurate results in this type di structures as well as the classical models. The main assumption of these methods is that the cross section (so also the ribs) *are rigid within their planes*. In fig.11 the deformed shape of the wing box is showed. Dashed lines are the edges of the undeformed shape instead the continuous lines represent the deformation.

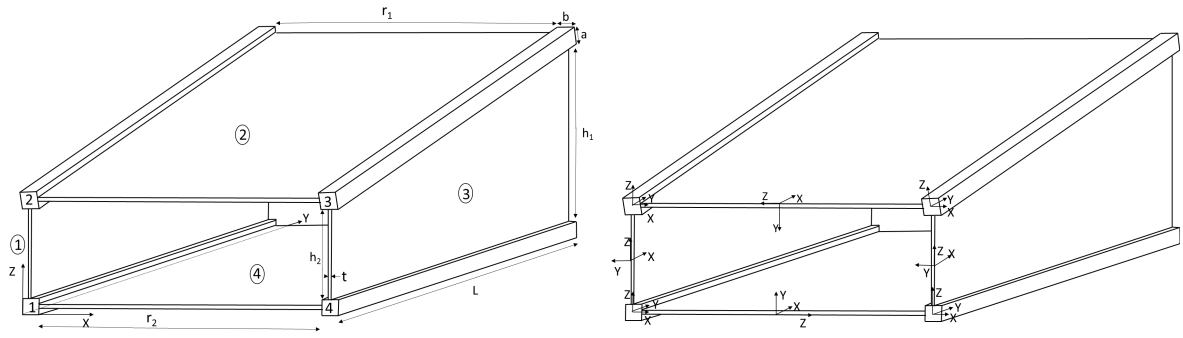

(a) Wing Box (b) 1D formulation

Figure 8. Tapered formulation.

Table 4. Displacement $w[m]$ of the center tip point of the stiffener .

	DOF	Point 1	Point 2	Point 3	Point 4
20L9	7296	-0.0185	-0.0191	0.00312	0.00312
Solid	58560	-0.0187	-0.0195	0.00319	0.00319
Beam+Shell	37700	-0.0229	-0.0238	0.00367	0.00367

These results show how the LE models used in this analysis provide results more similar to solid model compared to a model that merges both the 1D elements and 2D elements.

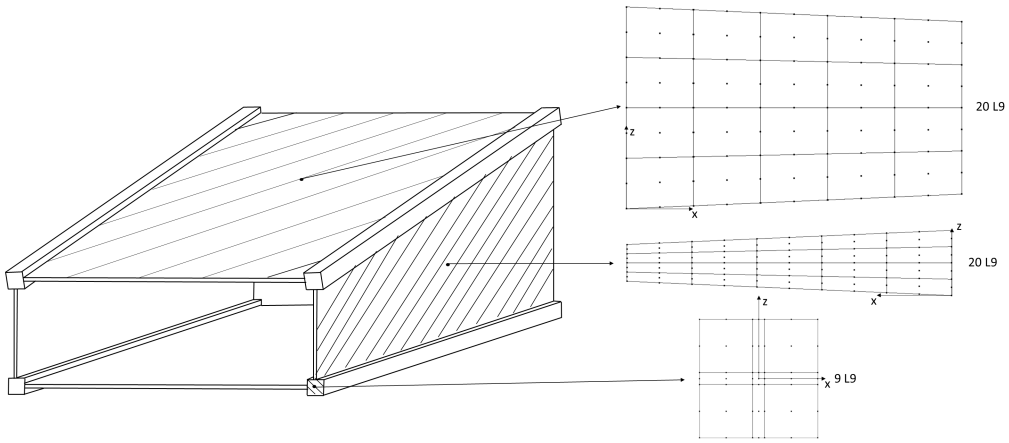

Figure 9. Cross-section L9 distributions for the wing box.

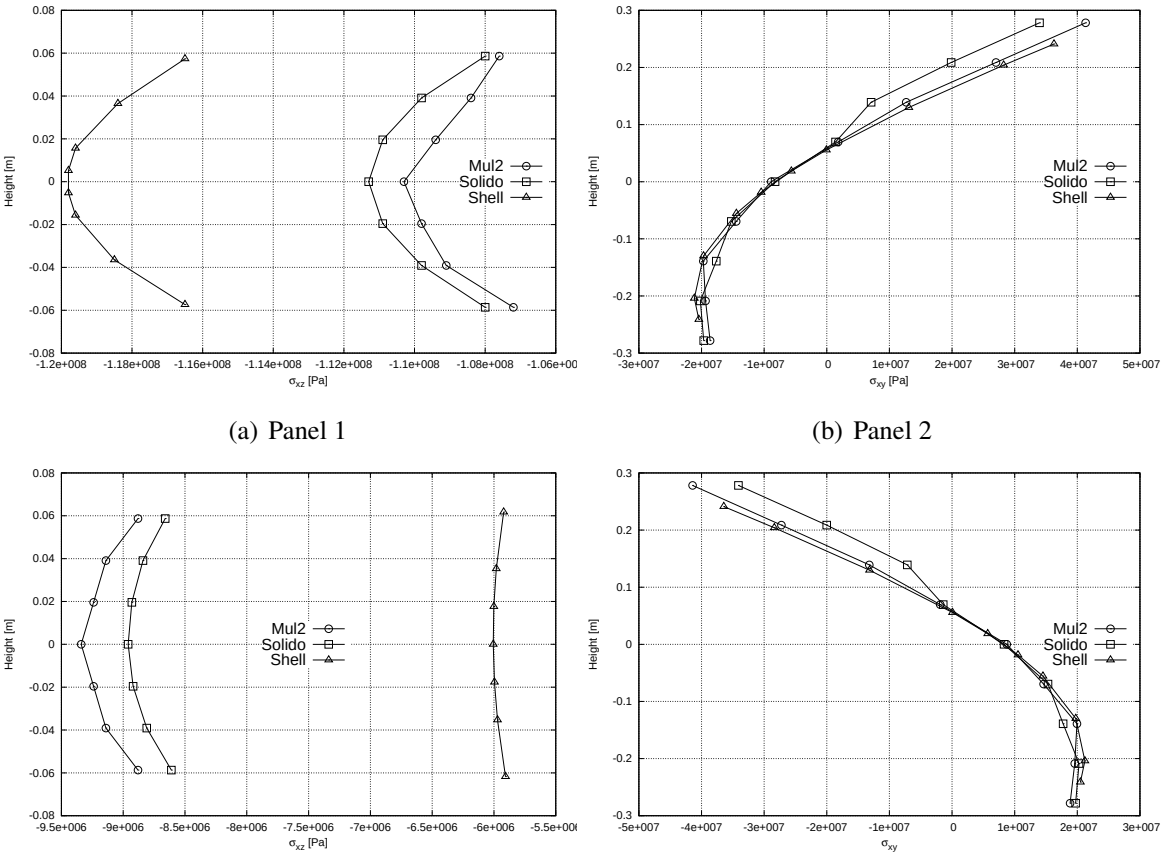

(a) Panel 1 (b) Panel 2

(c) Panel 3 (d) Panel 4

Figure 10. Trend of τ_{xz} and τ_{xy} vs panel height.

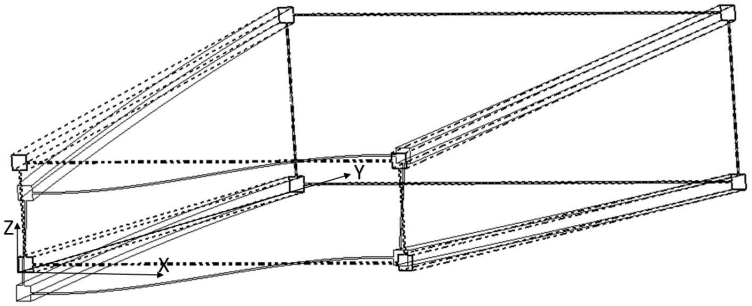

Figure 11. Deformed shape of wing box.

3.4 Tapered Wing Box with rib

In this case a rib on the tip is introduced. The load case is the same. The geometry of the rib is showed in fig.13 which presets the L9 distributions too. The thickness is equal to the thicknesses of the panels. Figure12 presents the geometry and the formulations used in this section. As for the panel, the rib has the *beam axis* along the thickness. Table 5 shows the displacements of the same points of the previous wing box. The table 6 show the average value of the shear stresses in the middle plane of the panel. Instead fig.14 shows the values of these stresses.

In the fig.15 the function of the rib can be appreciated.

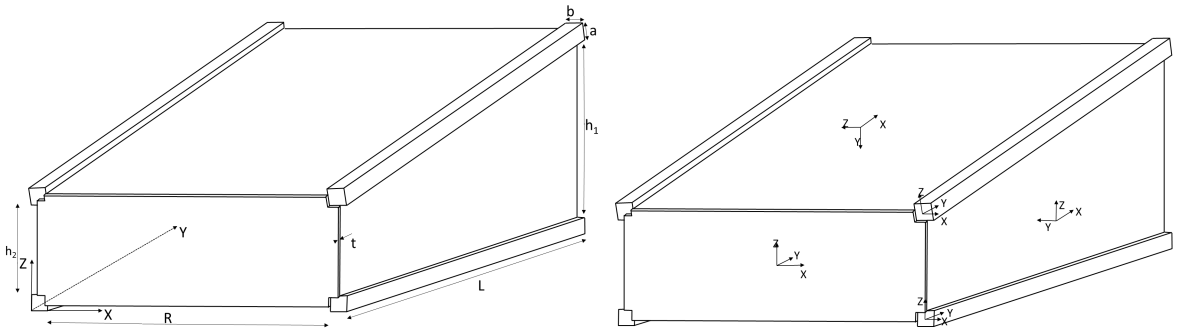

(a) Wing Box (b) 1D formulation

Figure 12. Tapered formulation.

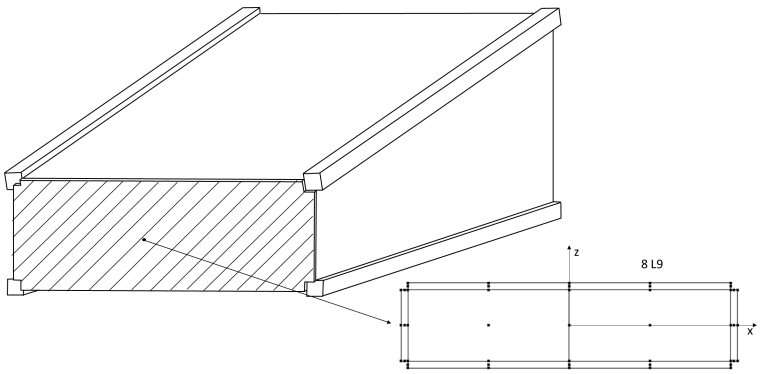

Figure 13. Cross-section L9 distributions for the rib.

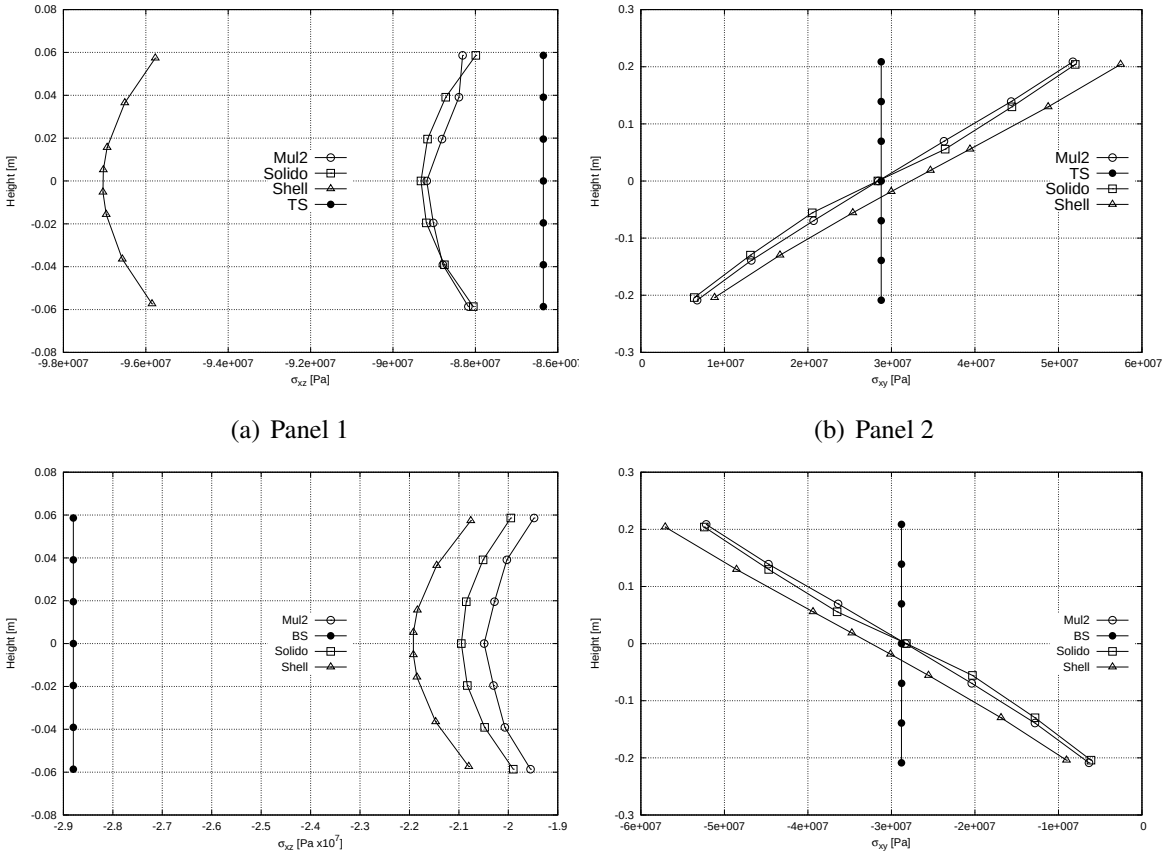

(a) Panel 1

(b) Panel 2

(c) Panel 3

(d) Panel 4

Figure 14. Trend of τ_{xz} and τ_{xy} vs panel height.

Table 5. Displacement $w[m]$ of the center tip point of the stiffener .

	DOF	Point 1	Point 2	Point 3	Point 4
20L9	9603	-0.0100	-0.0104	-0.0054	-0.0054
Solid	60831	-0.0101	-0.0106	-0.0055	-0.0055
Beam+Shell	43580	-0.0125	-0.01310	-0.0067	-0.0067

Table 6. Average τ_{ij} on the panel at $y = L/2$ and $x = t/2$.

	DOF	τ_{xz} [Pa] Panel 1	τ_{xy} [Pa] Panel 2	τ_{xz} [Pa] Panel 3	τ_{xy} [Pa] Panel 4
BF		-8.635	2.878	-2.878	-2.878
20L9	9603	-8.856	2.890	-1.989	-2.888
Solid	60831	-8.862	2.881	-2.041	-2.877
Beam+Shell	43580	-9.654	3.279	-2.129	3.279

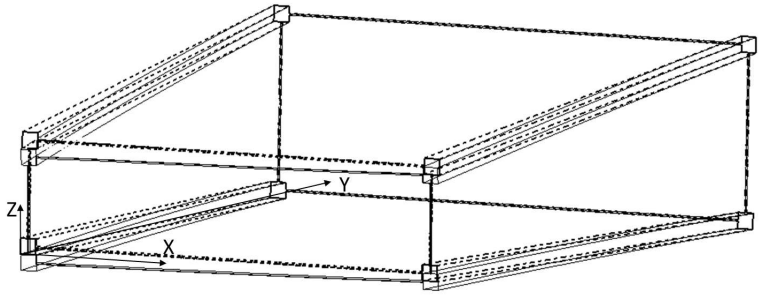

Figure 15. Deformed shape of wing box.

4. CONCLUSIONS

In this document different configurations of reinforced structures are take into account. For each structure a static analysis under a simple load case is performed through the use of a finite elements approach based on CUF. The cases show as LE formulation is useful for describe a multi-components structure and allows to know the behaviour of each component separately. Moreover, this work shows the capability of these formulations to model tapered shape without incurring in low accuracy results. From this work some main feature can be summarized in the following list:

- through the use of these *High Fidelity Reduced* models, any geometry can be represented without introducing approximations;
- results very close to those 3D can be achieved thanks the capability to have a deformable cross-section;
- this method can deal tapered structures. Moreover, complex structures can be described;
- the results obtained is better than those from the typical methods used in these analyses as the 1D model and 2D model.

References

[1] E. F. Bruhn. *Analysis and Design of Flight Vehicle Structures.* Tri-State Offset, Cincinnati, 1973.

[2] E. Carrera. *Fondamenti sul Calcolo di Strutture a Guscio Rinforzato per Veicoli Aerospaziali* Levrotto & Bella, Turin, Italy, 2011.

[3] J. M. Argyris, S. Kesley. *Energy Theorems and Structural Analysis* Butterworths Scientific Publ., London, 1960.

[4] E. Carrera. Theories and Finite Elements for Multilayered Plates and Shells: A Unified Compact Formulation with Numerical Assessment and Benchmarking. *Archives of Computational Methods in Engineering* Vol. 10, No. 3, 2003, pp. 216–296.

[5] Carrera E., Giunta G. and Petrolo M.. *Beam Structures: Classical and Advanced Theories* Advanced Theories, Wiley, New York, NY, 2011.

[6] Carrera E., Cinefra M., Petrolo M., and Zappino E.. *Finite Element Analysis of Strcture through Unified Formulation* John Wiley & Sons Ltd, 2014.

[7] Carrera E., Pagani A. and Petrolo M.. Classical, Refined, and Component-Wise Analysis of Reinforced-Shell Wing Structures. *AIAA JOURNAL* Vol. 51, No. 5, May 2013

[8] Carrera E., Filippi M., Zappino E.. Free vibration analysis of laminated beam by polynomial, trigonometric, exponential and zig-zag theories. *Journal of Composite Materials* 48(19), pp. 2299-2316, 2014

[9] Carrera E., Filippi M., Zappino E.. Laminated beam analysis by polynomial, trigonometric, exponential and zig-zag theories. *European Journal of Mechanics A/Solids* 41, pp. 58-69, 2013